# N-Heterocyclic Olefins as Ancillary Ligands in Catalysis: A Study of their Behaviour in Transfer Hydrogenation Reactions

Amaia Iturmendi, Nestor García, E. A. Jaseer, Julen Munárriz, Pablo J. Sanz Miguel, Victor Polo, Manuel Iglesias,* and Luis A. Oro*

The Ir(I) complexes [Ir(cod)(κP,C,P'-NHOPPh2)]PF6 and [IrCl(cod)(κC-NHOOMe)] (cod = 1,5-cyclooctadiene, NHOPPh2 = 1,3-bis(2-(diphenylphosphanyl)ethyl)-2-methyleneimidazoline) and NHOOMe = 1,3-bis(2-(methoxyethyl)-2-methyleneimidazoline), both featuring an N-heterocyclic olefin ligand (NHO), have been tested in the transfer hydrogenation reaction, this representing the first example of the use of NHOs as ancillary ligands in catalysis. Pre-catalyst [Ir(cod)(κP,C,P'-NHOPPh2)]PF6 has shown excellent activities in the transfer hydrogenation of aldehydes, ketones and imines using iPrOH as hydrogen source, while [IrCl(cod)(κC-NHOOMe)] decomposes throughout the reaction to give low yields of the hydrogenated product. Addition of one or two equivalents of a phosphine ligand to the latter avoids catalyst decomposition and significantly improves the reaction yields. The reaction mechanism has been investigated by means of stoichiometric studies and theoretical calculations. The formation of the active species ([Ir(κP,C,P'-NHOPPh2)(iPrO)]) has been proposed to occur via isopropoxide coordination and concomitant COD dissociation. Moreover, throughout the catalytic cycle the NHO moiety behaves as a hemilabile ligand, thus allowing the catalyst to adopt stable square planar geometries in the transition states, which reduces the energetic barrier of the process.

Introduction

N-Heterocyclic olefins (NHOs) feature strongly polarised double bonds due to the presence of two geminal amine substituents incorporated into a five-membered heterocycle. The aromatisation of the ring favours charge separation at the olefin, hence, ylidic mesomeric forms gain more weight (Scheme 1). As a result of this unique electronic structure, the terminal carbon of the NHO possesses a lone pair of electrons, which accounts for the nucleophilic nature of this type of molecules. NHOs, consequently, are able to react with Lewis acids such as, boranes, carbon dioxide and Group 14 adducts.[1]
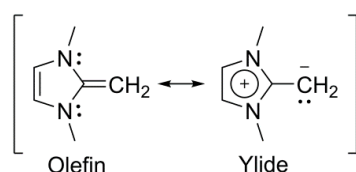
Scheme 1 Extreme resonance structures of a generic NHO.

Moreover, they can act as ligands for transition metal complexes, namely, Au, Rh, Ir and Mo have been reported.[2,1d] In this regard, it has been recently proved that NHCs are more strongly coordinating ligands than NHOs. In an elegant experiment that makes use of IR spectroscopy, structural data (X-ray crystallography) and DFT calculations, Rivard et al. compared the nature of the M–C bond and the donor capability of *N*-heterocyclic carbene (NHC) and N-heterocyclic olefin (NHO) ligands in [RhCl(CO)2L] complexes (where L = NHC or NHO). NHO ligands bring about lower carbonyl stretching frequencies, which is indicative of a higher electronic density at the metal centre. However, such behaviour is not the consequence of NHOs being more strongly σ-donating ligands than NHCs, but it has been attributed to a reduced π-acceptor ability in the case of NHOs; which, overall, results in weaker M–C bonds in the case of NHOs.[3]

The restricted number of transition metal complexes featuring NHO ligands so far described and the limited knowledge of their coordination chemistry has probably precluded their use in catalysis, since, to our best knowledge, no study of the catalytic activity of this class of complexes has been hitherto reported. Conversely, they have been employed as organocatalysts for a variety of reactions, often outperforming the widely successful NHCs.[4]

According to recent theoretical calculations at the DFT level[2c] the HOMO orbital of the NHO corresponds mainly to the lone pair at the p atomic orbital of the terminal carbon atom; whereas the HOMO–1 orbital would largely correspond to the double bond. The coordinated NHO shows values of the Wiberg bond index (WBI) between 1.14 and 1.22, which indicates that the ligand would be better represented by the ylidic mesomeric structure depicted in Scheme 1, i.e. the donation to the metal centre would take place by the HOMO orbital. Notwithstanding, the fact that the WBI depends on the nature of the complex points out that intermediate situations, where a certain degree of electron density is donated by the HOMO–1 orbital, are also conceivable. This unusual attribute allows NHO ligands to adapt to different coordination geometries, which may be of interest in catalytic processes. In this regard, we recently published various Ir complexes featuring the PC(NHO)P ligand 1,3-bis(2-(diphenylphosphanyl)ethyl)-2-methyleneimidazoline, which is

able to adjust to facial or meridional coordination modes depending on the steric requirements of the complex.[2c]

In this work we explore the performance of Ir-NHO complexes in catalysis using the transfer hydrogenation reaction as a test bench. Moreover, a theoretical study of the reaction mechanism, supported by experimental evidences, was performed in order to shed light on the behaviour of the NHO ligand throughout the catalytic cycle.

Results and discussion

The catalytic activity of the Ir(I) complexes [Ir(cod)(κP,C,P'-NHO^{PPh2})]PF$_6$ (**2**) and [IrCl(cod)(κC-NHO^{OMe})] (**5**) (cod = 1,5-cyclooctadiene; NHO^{PPh2} = 1,3-bis(2-(diphenylphosphanyl)ethyl)-2-methyleneimidazoline); NHO^{OMe} = 1,3-bis(2-(methoxyethyl)-2-methyleneimidazoline) was tested in the transfer hydrogenation of aldehydes, ketones and imines employing ^{i}PrOH as a hydrogen source. This work represents the first study of the behaviour of N-heterocyclic olefins (NHOs) as an ancillary ligand in catalysis. In order to evaluate the impact of the coordinating ability of the NHO's wingtip groups we tested two different complexes (**2** and **5**), which feature PPh$_2$ and OMe as potential donor groups, respectively.

The preparation and characterisation of complexes **1** and **2** (Scheme 2), where NHO^{PPh2} acts as a tridentate ligand, was previously reported by us.[2c]
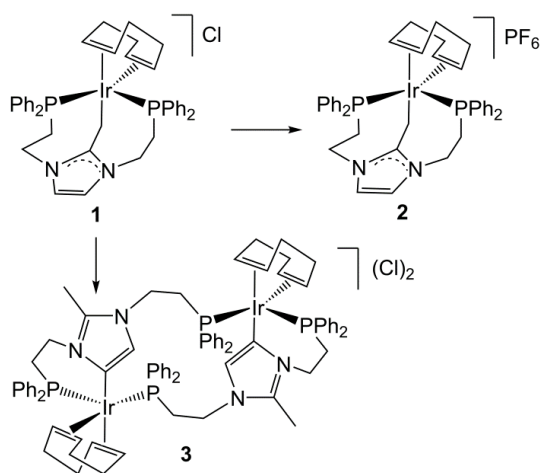
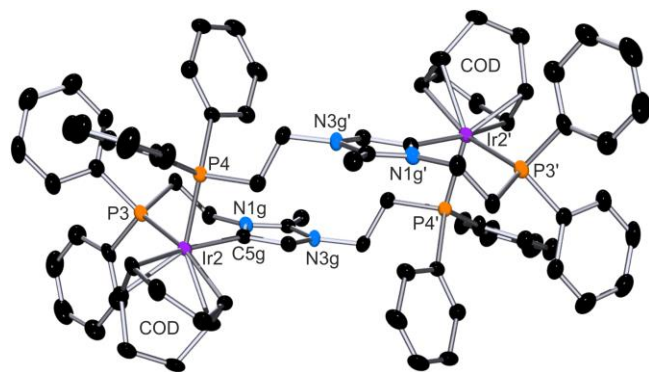**Scheme 2** Synthetic route to complexes **2** and **3**.

Figure 1 View of the cation of **3**. Selected bond lengths [Å] and angles [º] of **3**: Ir1–C5A, 2.088(7); Ir1–C5F, 2.157(7); Ir1–C6F, 2.162(8); Ir1–C1F, 2.232(7); Ir1–C2F, 2.239(7); Ir1–P1, 2.3160(18); Ir1–P2, 2.4107(19); Ir2–C5G 2.075(6); Ir2–C5L, 2.160(7); Ir2–C6L,

2.165(7); Ir2–C1L, 2.230(6); Ir2–C2L, 2.244(7); Ir2–P3, 2.3113(17); Ir2–P4, 2.4153(18); C5A–Ir1–P1, 90.26(19); C5A–Ir1–P2, 91.59(19); P1–Ir1–P2, 98.71(6);C5G–Ir2–P3, 90.58(18); C5G–Ir2–P4, 90.86(18); P3–Ir2–P4, 98.20(6).

We have recently observed that above 40 ºC **1** dimerises in CH$_2$Cl$_2$ to give binuclear complex **3** (Scheme 2), which crystallises from the reaction mixture (Figure 1). The unit cell of **3** encloses two different centrosymmetric cations,[5] which exhibit minor differences due to the accommodation of the C-rings (Ir1···Ir1', 8.6082(7) Å; Ir2···Ir2', 8.6430(7) Å).

The dimerisation process requires the dissociation of one of the wingtip groups in complex **1** to coordinate to a second iridium atom in complex **3**, thus acting as a bridging ligand in the new complex. Remarkably, the NHO ligand in **1** undergoes an isomerization process to give a C4 bound imidazolylidene ligand ("abnormal N-heterocyclic carbene") featuring a methyl group in the C2 position.

The ^{31}P NMR spectra of **3** in CD$_3$CN at temperatures above 313 K show two doublets for the two inequivalent phosphine ligands mutually coupled ($^2J_{P-P}$ = 29.7 Hz) at δ values of −18.6 and −26.1 ppm. However, at lower temperatures a new pair of doublets emerges at δ values of −17.4 and −20.7 ppm ($^2J_{P-P}$ = 29.7 Hz) that can be attributed to a different conformer of **3**. The ^{31}P NMR spectra in CD$_2$Cl$_2$ show again the presence of two pairs of doublets but, in this case, the minor conformer is present in higher proportions and, at temperatures above 323 K, the peaks disappear due to the decomposition of the complex. The ^{1}H NMR spectra of **3** show a complicated mixture of broad multiplets between approximate δ values of 4.50 and 1.50 ppm that correspond to the COD ligands and the methylenic protons of the wingtip groups of both conformers. Similarly, the broad multiplets that appear in the aromatic region are assigned to the phenyl rings of the phosphine moieties. The CH protons of the imidazole ring come about in a cleaner region, at δ values of ca. 6 ppm in CD$_3$CN. The fluxionality of **3** precluded its characterisation by ^{13}C NMR since the spectra in CD$_3$CN or CD$_2$Cl$_2$ show only some of the expected resonances as broad peaks even at low temperature.

In sharp contrast with **1**, complex **2**, which presents a PF$_6^-$ conterion instead of a Cl$^-$, does not experience any apparent modification of its structure at high temperatures. When a solution of **2** in CD$_3$CN is heated to 80 ºC no changes are observed in the ^{1}H or ^{31}P NMR spectra of the complex apart from the presence of small amounts of free COD. Hence, complex **2** was tested in transfer hydrogenation instead of **1** in order to ensure the molecular integrity of the catalyst.

A related iridium complex containing the new ligand of formula [IrCl(cod)(κC-NHO^{OMe})] (NHO^{OMe} = 1,3-bis(2-(methoxyethyl)-2-methyleneimidazoline) (**5**), was prepared NHO^{OMe} in order to assess the effect of the potential coordinating ability of the ligand's wingtip groups in the transfer hydrogenation of polar bonds.

The synthesis of the ligand precursor NHO^{OMe}·HCl (**4**) was achieved in two steps. First, 2-methylimidazole was deprotonated with sodium hydroxide in acetonitrile and reacted with 1 equivalent of 2-chloroethyl methyl to give the substituted imidazole, which was reacted neat with excess 2-

chloroethyl methyl ether to afford the product as an off-white solid in good yields. The ^{1}H NMR spectra of **4** show two singlets at δ values of 3.20 and 2.67 ppm that integrate 6 and 3 protons, respectively, which correspond to the CH$_3$O and CH$_3$ moieties. The CH$_2$N and CH$_2$O protons appear as triplets ($^3J_{H-H}$ = 4.7 Hz) at δ values of 4.45 and 3.67 ppm, respectively. Finally, only one singlet at a δ value of 7.74 ppm is observed for the aromatic CH protons due to the two-fold symmetry of the molecule.

The ligand, NHO^{OMe}, was generated in situ by deprotonation of **4** with 1 equivalent of potassium tert-butoxide in THF. Subsequently, the metal precursor [Ir(μ-Cl)(COD)]$_2$ was dissolved in toluene and added dropwise to the solution of NHO^{OMe} previously prepared. The inorganic salts were filtered off, the solvent was evaporated and the crude was washed repeatedly with hexane to afford complex **5** as a yellow solid in good yields (Scheme 3). In the ^{1}H NMR of complex **5**, two triplets ($^3J_{H-H}$ = 4.8 Hz) at δ values of 3.66 and 3.36 ppm are observed for the CH$_2$N and CH$_2$O groups, respectively. Besides, the two aromatic CH and OCH$_3$ protons of the NHO ligand come about as singlets at δ values of 6.26 and 2.92 ppm, which suggests that, in contrast to complexes **1** and **2**, the wingtip groups are not coordinated to the iridium centre. Therefore, the NHO ligand may rotate without barrier around the Ir–C bond at room temperature or adopt a fixed position below the chlorine atom (or the COD olefin), with the imidazolium ring being bisected by the Ir–Cl bond.
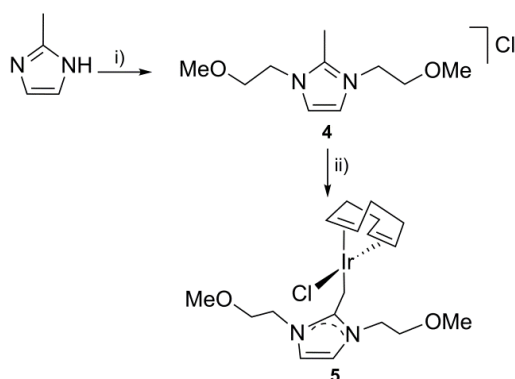

Scheme 3 Synthetic route to complex **5**; i) NaOH and ClCH$_2$CH$_2$OCH$_3$ in CH$_3$CN at 80 ºC for 18 h; ii) K^{t}BuO and [IrCl(COD)]$_2$ in THF at room temperature for 18 h.

Variable temperature ^{1}H NMR in toluene-d$_8$ shows a broadening of the methylenic and aromatic protons of the ligand at low temperatures, which suggests an unrestricted rotation around the Ir–C bond at room temperature that becomes more hindered at lower temperatures.

The olefinic protons of the COD ligand appear as two broad singlets at δ values of 4.59 and 3.27 ppm, evidencing the presence of two different ligands in *trans* position, namely, the NHO and Cl ligands. Noteworthy, the CH$_3$ group of the ligand precursor (**4**) disappears and a new resonance, a singlet that corresponds to the Ir–CH$_2$ protons, emerges at a δ value of 2.18 ppm. The ^{13}C NMR spectra of **5** show as the most representative resonances those assigned to the Ir–CH$_2$ and the NCN carbon atoms of the NHO ligand at δ values of 17.9 and 163.2 ppm, respectively.

In order to test the stability of the monodentate NHO complex, a solution of **5** in toluene-d$_8$ was placed in an NMR spectrometer and the temperature increased progressively. At temperatures above 60 ºC the formation of a new complex was observed. An increase of the reaction temperature to 70 ºC permits to achieve total conversion after 3 h (Scheme 4). The new complex, [IrCl(cod)(*a*NHC^{OMe})] (**6**) (*a*NHC^{OMe} = 1,3-bis(2-(methoxyethyl)-2-methylimidazole-4-ylidene), was identified as the result of an isomerisation NHO → *a*NHC (*a*NHC = abnormal *N*-heterocyclic carbene[6]) while the fragment "IrCl(cod)" remained unaffected, which agrees with the fact that NHCs are more strongly coordinating ligands than NHOs.[3] The ^{1}H NMR spectra of **6** show four different resonances for the methylenic protons of the wingtip groups, which appear as apparent triplets at δ values of 4.56, 3.93, 2.98 and 2.81 ppm. This contrasts with the ^{1}H NMR spectra of **5**, since only two resonances are observed for the side arms due to the two-fold symmetry of the complex. Analogously, the singlet resonance observed for the CH$_3$O protons in **5** disappears and two new singlets emerge at δ values of 3.03 and 2.77 ppm.

Further proof for the proposed isomerisation process lies on the integration of the low field peak at a δ value of 6.15 ppm that corresponds to the imidazole CH, which confirms the presence of only one aromatic proton. Besides, a new singlet that integrates 3 protons, corresponding to the methyl group at the imidazole ring, comes up at a δ value of 1.73 ppm, with concomitant loss of the Ir–CH$_2$ peak of complex **5**. The ^{13}C NMR spectra present as most representative resonances those corresponding to the Ir–C$_{Im}$ and C$_{Im}$–H carbon atoms that appear at δ values of 161.0 and 120.8 ppm, respectively.
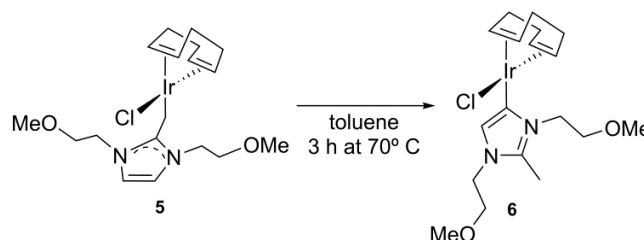
Scheme 4 Thermal isomerisation of **5** to yield **6** (NHO → *a*NHC).

It is worth mentioning that the isomerisation process is not reversible and complex **5** is not obtained again when the reaction mixture returns to room temperature; moreover, complex **6** remains unaltered at least until temperatures as high as 90 ºC in a toluene solution.

Attempts to abstract the chloride ligand with AgPF$_6$ in dichloromethane in order to form the *O*-coordinated chelate complex have been unsuccessful, probably due to the weak coordination of the ether functions, which precluded its isolation as a result of complex decomposition.

Catalysis

The transfer hydrogenation of carbonyl compounds and imines is a sustainable alternative to stoichiometric reduction reagents, and a less hazardous route to amines and alcohols than the catalytic hydrogenation with molecular hydrogen.[7] Therefore, owing to the importance of the reduction of C=O and

C=N bonds to the pharmaceutical industry, the development of more active catalysts for transfer hydrogenation, as well as the search for a better understanding of the mechanisms involved therein, are still ongoing endeavours. Moreover, the large number of iridium catalysts hitherto screened for this reaction makes it an excellent test bench to measure the activity of Ir-NHO complexes.[8,7c]

The catalytic activity of complex [Ir(PCP)(cod)]PF$_6$ (**2**) in transfer hydrogenation was studied for a variety of substrates, including, ketones, aldehydes and imines. The reaction conditions entailed the use of isopropanol as solvent, potassium *tert*-butoxide as a base and complexes **2** or **5** as catalysts at 80 ºC (a 1/5 ratio precatalyst/base was employed). Before addition of the substrate, the mixture precatalysts/base was preactivated in isopropanol by placing the mixture for 15 min in a thermostated oil bath at 80 ºC (Scheme 5). Subsequently, the reactions were monitored by GC analysis taking 0.1 mL aliquots at adequate reaction times using mesitylene as internal standard.

Under the conditions described above, we found that the catalytic transfer hydrogenation of cyclohexanone to cyclohexanol using 1 mol % of **2** is completed in 7 min with a TOF value of 2222 h^{-1} (Table 1, Entry 1). When the catalyst loading was reduced to 0.1 mol % the reaction time required to achieve total conversion was 5 h but, remarkably, a TOF value of 18750 h^{-1} was obtained (Table 1, Entry 2). These results compare well with the most active catalyst hitherto reported for the hydrogenation of cyclohexanone.[8b,f,j,k] For example, nanotube-supported [Ir(Cl)(COD)(NHC)] complexes give initial TOF values up to 5500 h^{-1} and 94% conversion in 80 min.[8k] Among the variety of substituted acetophenone derivatives screened for transfer hydrogenation, the unsubstituted acetophenone experienced the fastest transformation, rendering total conversion after 1 h (TOF = 779 h^{-1}) (Table 1, Entry 3).
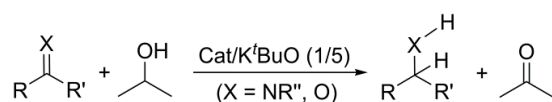
Scheme 5 Transfer hydrogenation of polar bonds using isopropanol as hydrogen source.

Noteworthy, no relationship between the substitution of this substrate and the catalytic activity can be drawn from these results. The use of aliphatic ketones increases the reaction times compared to their aromatic counterparts; namely, 3-decanone required 8.5 h of reaction to achieve a 79% conversion with a TOF value of 157 h^{-1} (Table 1, Entry 8).

The reduction of aldehydes by transfer hydrogenation presents inherent complications, such as, aldehyde decarbonylation followed by deactivation of the catalysts due to carbon monoxide coordination or to the formation of condensation by-products via aldehyde deprotonation. Remarkably, the transfer hydrogenation of benzaldehyde to benzyl alcohol using catalyst **2** was completed in 40 s with a TOF value of 16071 h^{-1} (Table 1, Entry 15).

Table 1 Transfer hydrogenation of ketones and aldehydes with catalyst **2**.

Entry	Substrate	T (min)	Conv. (%)	TOF$_{10\%}$ (h^{-1})
1		7	100	2222
2[a]		300	100	18750
3		60	100	779
4		90	100	1053
5		180	91	2143
6		180	100	594
7		60	100	319
8		510	79	157
9[b]		10	100	145
10		120	100	236
11[c]		30	100	166(**B**)
12[c,a]		420	100	259(**A**)/59(**B**)
13[c,d]		180	100	1948(**A**)/46(**B**)
14[c,e]		60	100	375(**A**)/31(**B**)
15		0.6	100	16071
16[a]		1440	63	28571

Conditions: catalyst (0.01 mmol), substrate (1 mmol), base (*t*BuOK, 0.05 mmol), *i*PrOH (5 mL), 80 ºC. Conv. determined by GC. [a] catalyst 0.001 mmol. [b] During the reaction mixtures of partially hydrogenated products are observed. [c] Mixtures of reduction products are obtained, 2-hydroxy-1,2-diphenylethanone (**A**) and 1,2-Diphenylethane-1,2-diol (**B**). [d] Catalyst (0.002 mmol). [e] 60 ºC.

A TOF value of 28571 h^{-1} was achieved when the catalyst loading was reduced to 0.1 mol %; however, total conversion to the alcohol was not accomplished (Table 1, entry 16), which suggests catalyst deactivation during the course of the reaction. To the best of our knowledge, the remarkable activity of this catalyst in the transfer hydrogenation of bezaldehyde is only surpassed by the Ru and Ir complexes reported by Baratta's and Xiao's groups, respectively.[9]

The hydrogenation of diketone 1,2-diphenylethane-1,2-dione (benzil) to the corresponding diol was completed in 30 min (TOF = 166 h^{-1}) using **2** as catalyst (Figure 2a). This reaction may afford two hydrogenation products, i.e the mono-hydrogenated product, 2-hydroxy-1,2-di(phenyl)ethanone (benzoin), and dihydrogenated product 1,2-diphenyl-1,2-ethanediol (hydrobenzoin), the latter being formed by hydrogenation of the former. After 5 min, the reaction

mixture contains 21% starting material, 64% benzoin and 15% hydrobenzoin. After 30 min, the starting material has been completely consumed, with a product distribution of 6% and 94% of benzoin and hydrobenzoin, respectively. After 90 min only hydrobenzoin is observed. The amount of catalyst was reduced to 0.2 mol % with the intention of reducing the reaction rate and, thus, allowing for the selective formation of benzoin (Figure 2b). In this case, after 45 min of reaction, there is a 36 % of benzil and a 64 % benzoin with no formation of hydrobenzoin. However, after 45 min, the formation of hydrobenzoin is initiated, which precludes total conversion to the mono-hydrogenated product. After 3 h, the starting material was completely consumed, with benzoin and hydrobenzoin being obtained in 31% and 69% yield, respectively. Reduction of the catalyst loading to 0.1 mol % afforded similar results to those obtained for 0.2 mol % (Figure 2c). After screening different catalyst loadings, the effect of the temperature on the selectivity was also studied. For that, the temperature was reduced to 60 °C (Figure 2d), with a 1 mol % of catalyst. After 15 min, the reaction mixture contains 25% of starting material and 75% of mono-hydrogenated product, benzoin. However, before total conversion to benzoin occurs, the mono-hydrogenated product starts to convert into the di-hydrogenated product. After 1 h, complete conversion to benzoin takes place. The transfer hydrogenation of imines usually proceeds more sluggishly than that of carbonyl compounds and significantly less examples are known.[10] Catalyst **2** shows good activities for the reduction of imines by transfer hydrogenation, for example, *N*-benzylideneaniline was transformed into *N*-benzylaniline using a 1 mol % of catalyst **2** in 45 min with a TOF value of 1118 h^{-1} (Table 2, Entry 1). Better TOF values were only achieved by the Ir(bis-NHC) catalysts described by Crabtree and Mieczknikowski,[7c] and improves the results obtained by Shvo's catalyst and other iridium catalysts.[11,8b] Substituted imines like *m*-methoxy-*N*-benzylideneaniline and *p*-methoxy-*N*-benzylideneaniline were also converted to their corresponding amines under the same reaction conditions, featuring TOF values of 584 h^{-1} and 110 h^{-1}, respectively (Table 2, Entries 3 and 4).

Complex **5** was tested in order to achieve a better understanding of the role played by the wingtip groups, and whether the presence of strongly coordinating functional groups would improve or hamper the activity of the catalyst. Initial catalytic tests were performed with cyclohexanone as the substrate. Complete conversion occurs after 2 h and the reaction shows a TOF value of 60 h^{-1} (Table 3, entry 1), which contrasts sharply with the results obtained with **2**, total conversion after 7 min and TOF = 2222 h^{-1} (Table 1, Entry 1).
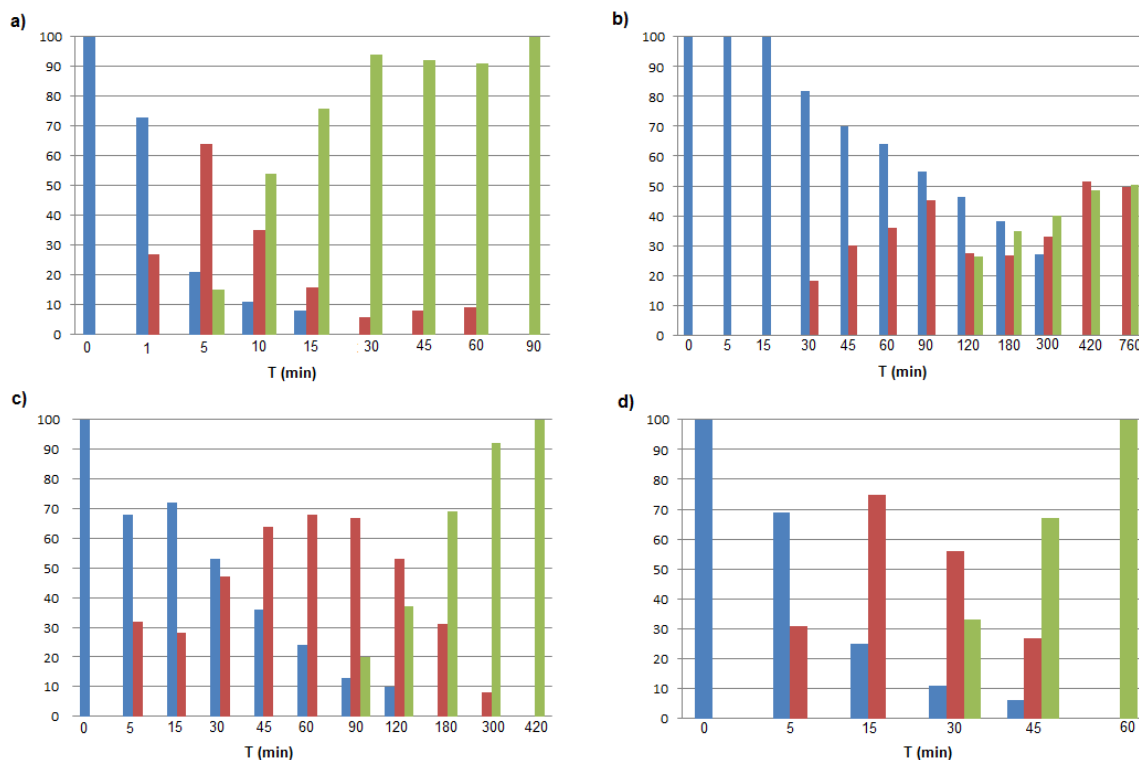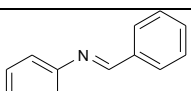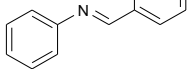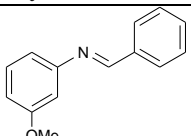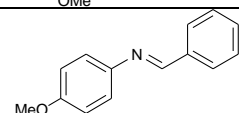

Figure 2 Hydrogenation of 1,2-diphenylethane-1,2-dione (blue) with catalyst **2** to the mono-hydrogenated product 2-hydroxy-1,2-di(phenyl)ethanone (red), and dihydrogenated product 1,2-diphenyl-1,2-ethanediol (green).

Table 2 Transfer hydrogenation of imines
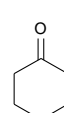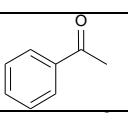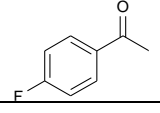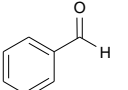
Entry	Substrate	Cat	T (min)	Conv (%)	TOF$_{10\%}$ (h^{-1})
1		**2**	45	98	1118
2		**5**[a]	1350	100	70
3		**2**	90	96	584
4		**2**	120	68	110

Conditions: catalyst (0.01 mmol), imine (1 mmol), base (*t*BuOK ,0.05 mmol), *i*PrOH (5 mL), 80 °C. Conv. determined by GC. [a] 2 eq P (*p*-F-C$_6$H$_4$)$_3$ were used as an additive.

Table 3. Transfer hydrogenation of ketones and aldehydes with catalyst **5**.

Entry	Substrate	Additive	T (min)	Conv. (%)	TOF$_{10\%}$ (h^{-1})
1		-	120	100	60
2		PPh$_3$ (1 eq)	15	100	822
3		PPh$_3$ (2 eq)	10	100	462
4		PCy$_3$ (2 eq)	25	100	513
5		P(*p*-F-Ph)$_3$ (2 eq)	5	100	3158
6		P(*p*-MeO-C$_6$H$_4$)$_3$ (2 eq)	10	100	2222
7		P(*o*-MeO-C$_6$H$_4$)$_3$ (2 eq)	120	100	99
8		P(*p*-Me-C$_6$H$_4$)$_3$ (2 eq)	10	100	984
9		P(*o*-Me-C$_6$H$_4$)$_3$ (2 eq)	30	100	181
10		P(*p*-F-C$_6$H$_4$)$_3$ (2 eq)	240	100	178
11		P(*p*-F-C$_6$H$_4$)$_3$ (2 eq)	120	100	171
12		PPh$_3$ (2 eq)	10	100	1905
13		P(*p*-F-C$_6$H$_4$)$_3$ (2 eq)	10	100	2222

Conditions: catalyst (0.01 mmol), substrate (1 mmol), base (*t*BuOK ,0.05 mmol), *i*PrOH (5 mL), 80 °C. Conv. determined by GC. [a] Catalyst 0.001 mmol.

Moreover, the formation of colloidal iridium is observed, which suggests that the catalyst progressively decomposes during the course of the reaction. With the intention of studying whether the addition of phosphine would improve the stability and activity of the catalyst, 1 equivalent of triphenylphosphine was added to the reaction mixture. Indeed, the new catalyst generated in situ led to complete conversion in 15 min with a TOF value of 822 h^{-1} (Table 3, entry 2).

When the amount of phosphine was increased to 2 equivalents, the reaction proceeded even faster, as it required only 10 min to reach complete consumption of cyclohexanone (Table 3, entry 3). With the intention of screening the effect of different phosphines in the activity of the in situ generated catalyst, P(*p*-F-Ph)$_3$, P(*p*-MeO-Ph)$_3$, P(*o*-MeO-Ph)$_3$, P(*p*-Me-Ph)$_3$, P(*o*-Me-Ph)$_3$ and PCy$_3$ (Cy = Cyclohexyl) were employed as additives (Table 3, Entries 3 to 9). Among them, the highest activity was obtained for tris(4-fluorophenyl)phosphine, P(*p*-F-Ph)$_3$, with a TOF value of 3158 h^{-1} (Table 3, Entries 5), whilst the least reactive catalytic system was that resulting from the use of tris(o-methoxyphenyl)phosphine (P(*o*-MeO-Ph)$_3$), which features a TOF value of 99 h^{-1} (Table 3, Entries 7). Hence, we used 2 equivalents of P(*p*-F-Ph)$_3$ with complex **5** for the screening of the transfer hydrogenation reaction with various substrates. In the case of acetophenone or benzaldehyde, the activity drops significantly compared to catalyst **2.** Complete conversion was achieved after 60 min with **2** (TOF = 779 h^{-1}) for acetophenone, while **5** required 240 min (TOF = 178 h^{-1}). The case of benzaldehyde is even more pronounced since catalyst **2** affords total conversion after 40 s (TOF = 16071 h^{-1}), being remarkably more active than **5** (with two equivalents of P(*p*-F-Ph)$_3$), which requires 10 min (TOF = 2222 h^{-1}) (Table 3, Entry 14). Similarly, *N*-benzylideneaniline is totally hydrogenated in 45 min with catalyst **2** (TOF = 1118 h^{-1}) while **5** with 2 equivalents of P(*p*-F-Ph)$_3$ as additive necessitates almost 24 h (TOF = 70 h^{-1}) (Table 2, Entry 2).

Mechanism

A theoretical study at the DFT level, using the B3LYP-D3 method, has been carried out in order to clarify some key points of the reaction mechanism for catalyst **2** employing acetophenone as a model substrate. First, the energetic cost for the decoordination of the different donor moieties of the PCP ligand or COD ligand (phosphine, NHO or olefin) upon coordination of *tert*-butoxide to **2** (structure **A**) has been evaluated (see Figure 3). Decoordination of one phosphine ligand to form a square planar Ir complex (**A1**) raises the relative energy 29.9 kcal/mol, and is, therefore, an unfeasible process. Alternatively, dissociation of the coordinated NHO leads to the coordination of the second olefin of the COD ligand, forming the trigonal bipyramid **A2** complex, which increases the energy 21.1 kcal/mol. Finally, complete decoordination of the COD ligand forming the square planar metallic complex **A3** is nearly isoenergetic (1.8 kcal/mol) than complex **A**. Therefore, COD dissociation is the most energetically favourable process. This is in agreement with experimental observations, since addition of 1 equivalent of sodium isopropoxide to a solution of **2** in methanol-d$_4$ affords the free COD upon heating to 80 °C. Besides, a mixture of two unidentified complexes, which show one singlet each in the ^{31}P NMR at δ values of 8.9 and –17.3 ppm, is also observed. In this regard, it is worth mentioning that none of the peaks corresponds to the free PCP ligand (–22.2 ppm) or the starting complex (**2**) (a broad singlet at –24.4 ppm). Following this line of thought, attempts to prepare a Rh complex analogous to **2** resulted always in COD dissociation. The ^{1}H NMR resonances that correspond to the free COD ligand appear at δ values of 5.55 and 2.35 ppm. The unsaturated complex thus obtained can be stabilised in a THF solution by solvent coordination. However,

attempts to isolate the THF adduct have been unsuccessful. The ^{31}P NMR spectrum in CD_2Cl_2 confirms that the PCP ligand remains coordinated to the rhodium centre, as it shows a doublet resonance due to P-Rh coupling ($^1J_{Rh-P}$ = 92.5 Hz) at a δ value of 2.43 ppm. Moreover, the methylenic protons of the wingtip groups are diastereotopic, 4 multiplets are observed centred at δ values of 4.56, 4.11, 3.62 and 3.44 ppm, which confirms the coordination of the NHO moiety. The higher tendency of the Rh complex to eject the COD ligand can be explained in terms of an increased steric hindrance about the metal centre due to the smaller size of rhodium compared to iridium.

Another evidence that supports the decoordination of the 1,5-cyclooctadiene ligand (COD) to form the active species is that neither catalysts **2** nor **5** catalyse the transfer hydrogenation of olefins, namely, cyclooctene, COD or styrene, which proves that the required vacant coordination sites need to be generated by a process different from COD hydrogenation. In fact, addition of excess COD (1 mL) to the reduction of cyclohexanone to cyclohexanol using **2** as catalyst completely inhibits its catalytic activity, probably due to the impossibility to generate the active species in significant amounts under these conditions.

The transfer hydrogenation of ketones may proceed via a stepwise mechanism by means of a hydride intermediate or a concerted one, also called the MPV (Meerwein–Ponndorf–Verley) mechanism. Although Ir complexes usually follow the monohydride route, both possible pathways have been calculated in order to clarify the role of the NHO ligand in the elementary steps of the catalytic cycle.[12] The calculated Gibbs free energy profile is shown in Figure 4 assuming decoordination of the COD ligand (starting from **A3**). An alternative energetic profile starting from **A** was also calculated; however, a significantly higher overall energy barrier was obtained (Supporting Information).

The stepwise mechanism starts by β-elimination of the C–H bond at the alkoxo ligand via transition state **TSB/C** to yield the hydride intermediate **C**, this step presents an activation energy of 22.3 kcal/mol. Remarkably, **TSB/C** features a dissociated NHO ligand, which allows the metal centre to adopt a square planar geometry. Exchange of acetone by acetophenone gives complex **D**, thus leading to the migratory insertion of the ketone into the Ir–H bond through transition state **TSD/E**. The activation energy of this step is 29.0 kcal/mol and, analogously to **TSB/C**, requires the decoordination of the NHO ligand from the metal centre. Finally, 1-phenylethanol is released through a proton transfer mechanism characterised by transition state **TSE/F** upon coordination of a molecule of ^{i}PrOH to the metal. Alternatively, the concerted MPV mechanism occurs via **TSB/E**, showing a relative energy of 34.9 kcal/mol.

The DFT calculated energetic profile reveals that the hydride intermediates are exergonic and the overall activation energy (29.0 kcal/mol) is determined by intermediate **D** and **TSD/E**. Noteworthy, the NHO moiety acts as a hemilabile ligand coordinating to the metal at the intermediates but decoordinating at the transition states. A plausible explanation for this behaviour would be that the reversible coordination of the NHO makes it possible for the iridium centre to preserve the more favourable square planar geometry throughout the reaction pathway, thus decreasing the energy of the corresponding transition states.

Conclusion

In summary, we have evaluated for the first time the behaviour of NHOs as ancillary ligands in catalysis. Several conclusions may be drawn from the experiments described here. Firstly, the NHO–Ir bond is labile and requires the coordination of the wingtip groups to stabilize this coordination mode. In fact, in this work we present the only examples so far reported an isomerization NHO → aNHC.
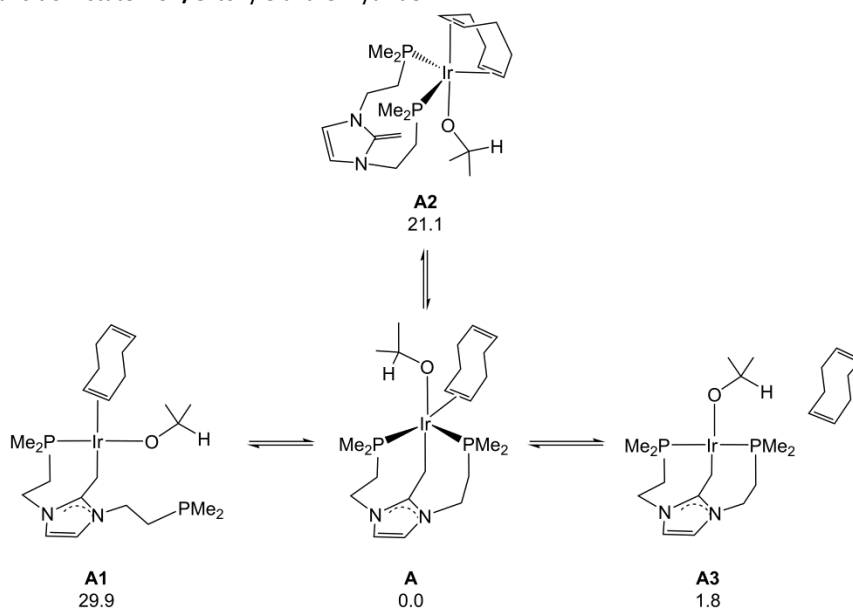

Figure 3 DFT calculated relative Gibbs free energy (to **A**, in kcal/mol) for the possible isomers of complex **2**[+] and iPrO[-].
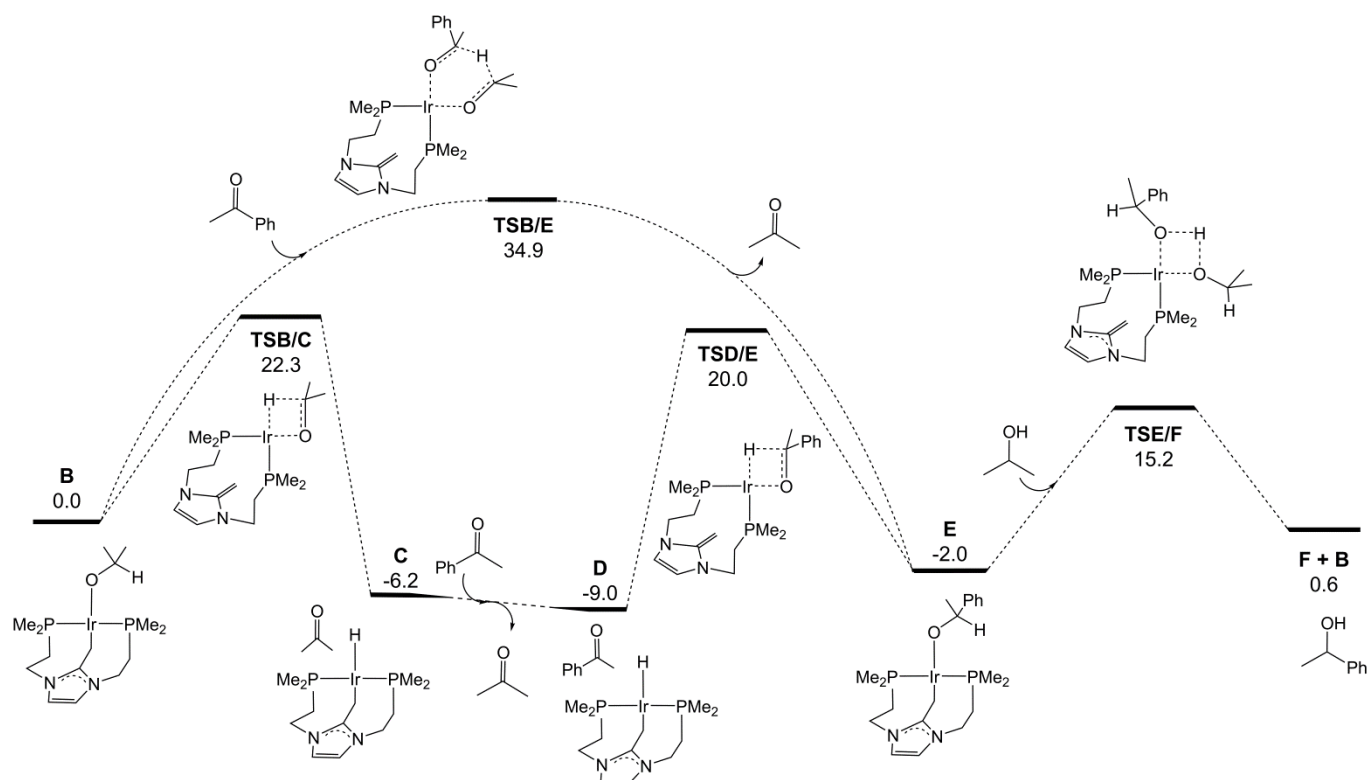
Figure 4 DFT calculated Gibbs free energy profile (relative to **B** and isolated molecules, in kcal/mol) for the stepwise and concerted transfer hydrogenation of ketones by 2-propanol catalysed by **2**.

Secondly, the decoordination of the COD ligand appears to be energetically more favourable than NHO dissociation in complex **2** and its rhodium analogue, both featuring two strongly coordinating side arms (two PPh₂ moieties). As a consequence of this behaviour, under catalytic conditions, i.e. in the presence of isopropoxide at 80 °C complex **2** is transformed into the active species [Ir(PCP)(ⁱPrO)]. via isopropoxide coordination and concomitant COD dissociation.

Finally, theoretical calculations at the DFT level support this postulation while, at the same time, show that the PCP ligand behaves as a hemilabile ligand. The NHO moiety is able to dissociate from the iridium centre in order to allow the catalyst to adopt square planar geometries at the transition states, which are more stable than the related tpb geometries, thus reducing the overall energetic barrier of the process.

Experimental

General Procedures

All the manipulations were performed using standard Schlenk techniques under an argon atmosphere. 2-Propanol of analytical grade used as hydrogen donor was dried with Molecular Sieves and degassed prior to use. Complex [Ir(COD)Cl]₂ was synthesised according to literature methods.[13] The substrates were obtain from common commercial sources and used as received. Air sensitive compounds were stored and weighed in a glovebox. All experiences have been carried out under argon atmosphere. NMR spectra were recorded on Bruker Avance 300 MHz spectrometer. Chemical shifts

are given as dimensionless δ values and are frequency referenced relative to residual solvent peaks for ¹H and ¹³C. All coupling constants J are given in Hertz and multiplicity of the signals is indicated as *s*, *singlet*; *d*, *doublet*; t, *triplet*; q, *quartet*; m, *multiplet*. Carbon, hydrogen and nitrogen analysis were performed using a Perkin-Elmer 2400 microanalyzer. The substrates were obtained from common commercial sources and used as received. Air sensitive compounds were stored and weighed in a glovebox.

General Procedure for Transfer Hydrogenation Catalysis. A solution of the corresponding catalyst precursor (0.01 mmol) and ᵗBuOK (5.6 mg, 0.05 mmol) in dry 2-propanol (5 mL) was prepared under argon in a 25 mL Schlenk flask. The solution was heated to 80 °C for 15 min in a thermostated oil bath before the addition of substrate (1 mmol) and the internal standard (mesitylene, 140 μL, 1 mmol). The resulting mixture was stirred at 80 °C and monitored by gas chromatography. Aliquots (0.3 mL) were taken at fixed times, quenched in tetrahydrofuran (1 mL) and filtered through a short path of SiO₂. Yields were determined by GC analysis of reaction mixtures using an Agilent Technologies 7890A. Column: Agilent J&W HP-5, 0.25 mm × 30m × 0.25 μm. Substrates identities were determined by NMR spectroscopy and GC-MS analysis using an Agilent Technologies 7890A system with an Agilent Technologies 5975C inert MS detector. Column: Agilent J&W DB-1. Experiments at different temperature using 1,2-diphenylethane-1,2-dione (benzil) were performed in the same manner.

1,3-bis(2-(methoxyethyl)-2-methylimidazolium chloride (4). 2-methylimidazole (3.3 g, 40 mmol) was added over a solution of

sodium hydroxide (3.2 g, 80 mmol) and 2-chloroethyl methy ether (40 mmol, 4 mL) in acetonitrile (20 mL). This solution was refluxed at 80 °C for 18 h. Then, the solution was filtered and the solvent evaporated under reduced pressure. The resulting oil was redissolved in 2-chloroethyl methyl ether (7 mL) and refluxed for 3 days at 90 °C. Evaporation of the volatiles afforded a brown oil that was washed with diethyl ether (3 x 10 mL) to give the product as an off-white solid (6.4 g, 27 mmol, 68% yield). ^{1}H NMR (300 MHz, CDCl$_3$): δ 7.74 (s, 2H, NCH), 4.45 (t, J_{H-H} = 4.7, 4H, CH$_2$N), 3.67 (t, J_{H-H} = 4.7, 4H, CH$_2$O), 3.20 (s, 6H, OCH$_3$), 2.67 (s, 3H, CH$_3$). ^{13}C(75 MHz, CDCl$_3$): δ 144.9 (s, NCN), 122.0 (s, NCH), 70.8 (s, CH$_2$O), 59.0 (s, OCH$_3$), 48.9 (s, CH$_2$N), 10.7 (s, CH$_3$). HRMS (ESI) m/z calcd. for C$_{10}$H$_{19}$N$_2$O$_2$Cl (M − Cl$^-$) 199.1441, found, 199.1443. Anal. Calcd. for C$_{10}$H$_{19}$N$_2$O$_2$Cl (234.72): C, 51.17; H, 8.16; N, 11.93. Found: C, 50.95; H, 8.05; N, 11.15.

Complex 5. Potassium tert-butoxide (225 mg, 2 mmol) was added to a solution of 1,3-bis(2-methoxyethyl)-2-methylimidazolium chloride (400 mg, 1.7 mmol) in tetrahydrofuran (10 mL). After 1 h a solution of bis(1,5-cyclooctadiene)diiridium(I) dichloride (600 mg, 0.89 mmol) in tetrahydrofuran (10 mL) was added dropwise to the first solution and stirred for 18 h at room temperature. The solvent was removed under reduced pressure and the solid dissolved in toluene (10 mL). The solution was filtered through Celite and the solvent removed under reduced pressure. The oil was washed with hexane (2 x 10 mL) and the product was obtained as a yellow solid (363 mg, 0.68 mmol, 40% yield). ^{1}H NMR (300 MHz, C$_6$D$_6$): δ 6.26 (s, 2H, NCH), 4.59 (bs, 2H, CH$_{COD}$), 3.66 (t, J_{H-H} = 4.8, 4H, CH$_2$N), 3.36 (t, J_{H-H} = 4.8, 4H, CH$_2$O), 3.27 (bs, 2H, CH$_{COD}$), 2.92 (s, 6H, CH$_3$), 2.45-2.27 (m, 4H, CH$_2$ $_{COD}$), 2.18 (s, 2H, CH$_2$Ir), 1.72–1.58 (m, 4H, CH$_2$ $_{COD}$) ^{13}C NMR (75 MHz, C$_6$D$_6$): δ 163.2 (s, NCN), 117.6 (s, NCH), 70.9 (s, CH$_{COD}$), 70.5 (s, CH$_2$O), 58.4 (s, CH$_3$), 52.7 (s, CH$_{COD}$), 47.4 (s, CH$_2$N), 33.9 (s, CH$_2$ $_{COD}$), 31.5 (s, CH$_2$ $_{COD}$), 17.9 (s, CH$_2$Ir). HRMS (ESI) m/z calcd. for C$_{18}$H$_{30}$IrN$_2$O$_2$Cl (M − Cl$^-$) 499.1932, found, 499.1928. Anal. Calcd. for C$_{18}$H$_{30}$IrN$_2$O$_2$Cl (534.16): C, 40.48; H, 5.66; N, 5.24. Found: C, 39.96; H, 5.64; N, 5.37.

Complex 6. A toluene solution of **5** (60 mg, 0.11 mmol) was heated for 3 h at 70 °C. Then, the solvent was removed under reduced pressure and the solid washed with hexane (3 x 10 mL). The product was obtained as a dark yellow solid (45 mg, 0.08 mmol, 75% yield). ^{1}H NMR (300 MHz, C$_7$D$_8$): δ 6.08 (s, 1H, NCH), 4.92-4.83 (bs, 2H, CH$_{COD}$), 4.52 (t, J_{H-H}=4.9, 2H, CH$_2$N), 3.89 (t, J_{H-H}=5.0, 2H, CH$_2$O), 3.09 (bs, 2H, CH$_{COD}$), 2.98 (s, 3H, OCH$_3$), 2.94 (t, J_{H-H}=5.1, 2H, CH$_2$N), 2.76 (t, J_{H-H}=5.1, 2H, CH$_2$O), 2.73 (s, 3H, OCH$_3$), 2.45-2.30 (m, 4H, CH$_2$COD), 1.83-1.72 (m, 4H, CH$_2$ $_{COD}$), 1.69 (s, 3H, CH$_3$). ^{13}C NMR (75 MHz, C$_7$D$_8$): δ 161.8 (s, IrC), 141.8 (s, NCN), 121.5 (s, NCH), 80.4 (s, CH$_{COD}$), 72.6 (s, OCH$_2$), 71.3 (s, OCH$_2$), 59.0 (s, OCH$_3$), 58.9 (s, OCH$_3$), 51.7 (s, CH$_{COD}$), 49.9 (s, NCH$_2$), 47.0 (s, NCH$_2$), 35.1 (s, CH$_2$ $_{COD}$), 31.0 (s, CH$_2$ $_{COD}$), 10.2 (s, CH$_3$). HRMS (ESI) m/z calcd. for C$_{18}$H$_{30}$IrN$_2$O$_2$Cl (M − Cl$^-$) 499.1932, found, 499.1927. Anal. Calcd. for C$_{18}$H$_{30}$IrN$_2$O$_2$Cl (534.16): C, 40.48; H, 5.66; N, 5.24. Found: C, 40.03; H, 5.25; N, 5.41.

Computational details

All DFT theoretical calculations have been carried out using the Gaussian program package.[14] The B3LYP method[15] has been employed including the D3 dispersion correction scheme developed by Grimme[16] for both energies and gradient calculations and the "ultrafine" grid. The def2-SVP basis set[17] has been selected for all atoms and the PCM method[18] was chosen to simulate solvent effects (2-propanol, ε=19.264), both have been used for geometry optimizations and calculation of Gibbs energy corrections at 298 K.

Single-point energy corrections using the def2- TZVP basis set have been included. The nature of the stationary points has been check by analytical frequency analysis and transition states were characterized by a single imaginary frequency corresponding to the expected motion of the atoms.

Notes and references

‡ Intermediates **C** and **D** are adducts of the square planar Ir(I) complex [IrH(κP,C,P'-NHO^{PPh2})] with acetone and acetophenone, respectively.
1 a) Y. Wang, M. Y. Abraham, R. J. Gilliard, Jr., D. R. Sexton, P. Wei and G. H. Robinson, *Organometallics* 2013, **32**, 6639–6642; b) S. M. I. Al-Rafia, A. C. Malcolm, S. K. Liew, M. J. Ferguson, R. McDonald and E. Rivard, *Chem. Commun.,* 2011, **47,** 6987–6989; c) N. Kuhn, H. Bohnen, J. Kreutzberg, D. Bläser and R. Boese, *J. Chem. Soc., Chem. Commun.*, 1993, 1136–1137; d) Y.-B. Wang, Y.-M. Wang, W.-Z. Zhang and X.-B. Lu, *J. Am. Chem. Soc.* 2013, **135**, 11996–12003; e) S. Kronig, P. G. Jones and M. Tamm, *Eur. J. Inorg. Chem.* 2013, 2301–2314.
2 a) A. Fürstner, M. Alcarazo, R. Goddard and C. W. Lehmann, *Angew. Chem.* 2008, **120**, 3254–3258; *Angew. Chem. Int. Ed.* 2008, **47**, 3210–3214; b) M. Viciano, M. Feliz, R. Corberán, J. A. Mata, E. Clot and E. Peris, *Organometallics* 2007, **26**, 5304–5314; c) M. Iglesias, A. Iturmendi, P. J. Sanz Miguel, V. Polo, J. J. Pérez-Torrente and L. A. Oro, *Chem. Commun.,* 2015, **51**, 12431–12434.
3 K. Powers, C. Hering-Junghans, R. McDonald, M. J. Ferguson, E. Rivard *Polyhedron* 2016, **108**, 8–14
4 R. D. Crocker and T. V. Nguyen, *Chem. Eur. J.* 2016, **22**, 2208–2213 (and references therein).
5 Crystal data of compound **3**: [C$_{84}$H$_{100}$Cl$_{10}$Ir$_2$N$_4$O$_2$P$_4$], triclinic, *P−1*, *a* = 13.9013(7) Å, *b* = 17.4906(9) Å, *c* = 20.0339(11) Å, *α* = 93.6950(10)º, *β* = 105.6320(10)º, *γ* = 110.4170(10)º, *Z* = 2, *M*$_r$ = 2060.46, *V* = 4327.9(4) Å^3, *D*$_{calcd}$ = 1.581 g cm^{-3}, *λ*(Mo Kα) = 0.71073 Å, T = 100 K, *μ* = 3.502 mm^{-1}, 52738 reflections collected, 20117 unique (*R*$_{int}$ = 0.0355), 16485 observed, *R*1(*F*$_o$) = 0.0576 [*I* > 2σ(*I*)], *wR*2 (*F*$_o$^{2}) = 0.1628 (all data), GOF = 1.043. CCDC 1487555.
6 O. Schuster, L. Yang, H. G. Raubenheimer and M. Albrecht, *Chem. Rev.*, 2009, **109**, 3445–3478.
7 a) F. A. Carey, R. J. Sundberg, Advanced Organic Chemistry, thirded., Part B: Reactions and Synthesis, Plenum Press, New York, 1990, p. 232; b) R. A. W. Johnstone, A. H. Wilby and I. D. Entwistle, *Chem. Rev.* 1985, **85**, 129–170; c) J. R.

Miecznikowski and R. H. Crabtree, *Polyhedron* 2004, **23**, 2857–2872.

8   For examples see: a) J. Campos, U. Hintermair, T. P. Brewster, M. K. Takase and R. H. Crabtree, *ACS Catal.* 2014, **4**, 973–985; b) M. V. Jiménez, J. Fernández-Tornos, J. J. Pérez-Torrente, F. J. Modrego, S. Winterle, C. Cunchillos, F. J. Lahoz and L. A. Oro, *Organometallics* 2011, **30**, 5493–5508; c) A. Binobaid, M. Iglesias, D. Beetstra, A. Dervisi, I. Fallis and K. J. Cavell, *Eur. J. Inorg. Chem.* 2010, 5426–5431; d) N. García, E. A. Jaseer, J. Munárriz, P. J. Sanz Miguel, V. Polo, M. Iglesias and L. A. Oro, *Eur. J. Inorg. Chem.* 2015, 4388–4395; d) M. Albrecht, J. R. Miecznikowski, A. Samuel, J. W. Faller and R. H. Crabtree, *Organometallics* 2002, **21**, 3596; e) J. R. Miecznikovski and R. H. Crabtree, *Organometallics* 2004, **23**, 629; f) A. C. Hillier, H. M. Lee, E. D. Stevens and S. P. Nolan, *Organometallics* 2001, **20**, 4246–4252; g) J. R. Miecznikowski and R. H. Crabtree, *Organometallics* 2004, **23**, 629–631; h) J.-W. Handgraaf, J. N. H. Reek and E. J. Meijer, *Organometallics* 2003, **22**, 3150–3157; i) R. Castarlenas, M. Esteruelas and A. E. Oñate, *Organometallics* 2008, **27**, 3240–3247; j) M. Blanco, P. Álvarez, C. Blanco, M. V. Jiménez, J. Fernández-Tornos, J. J.Pérez-Torrente, L. A. Oro and R. Menéndez, *ACSCatal.* 2013, **3**, 1307–1317; k) M. Blanco, P. Álvarez, C. Blanco, M. V. Jiménez, J. J. Pérez-Torrente, L. A. Oro, J. Blasco, V. Cuartero and R. Menéndez, *Catal. Sci. Technol.* DOI:10.1039/c5cy01998b.

9   a) W. Baratta, K. Siega and P. Rigo, *Adv. Synth. Catal.* 2007, **349**, 1633–1636; b) X. Wu, J. Liu, X. Li, A. Zanotti-Gerosa, F. Hancock, D. Vinci, J. Ruan and J. Xiao, *Angew. Chem., Int. Ed.* 2006, **45**, 6718–6722.

10 a) O. Saidi and J. M. J. Williams, *Top Organomet. Chem.* 2011, **34**, 77–106; b) J. Han, S. Kang and H. -K. Lee, *Chem. Commun.* 2011, **47**, 4004–4006; c) C. P. Casey, S. W. Singer, D. R. Powell, R. K. Hayashi and M. Kavana, *J. Am. Chem. Soc.* 2001, **123**, 1090–1100; d) G.-Z. Wang and J.-E. Bäckvall, *J. Chem. Soc., Chem. Commun.* 1992, 980–982; e) Y. Watanabe, Y. Tsuji, H. Ige, Y. Ohsugi and T. J. Ohta, *Org. Chem.* 1984, **49**, 3359–3363; f) M. Martín, E. Sola, S. Tejero, J. L. Andrés and L. A. Oro, *Chem. Eur. J.* 2006, **12**, 4046–4056; g) N. Fleury-Brégeot, V. De la Fuente, S. Castillón and C. Claver, *ChemCatChem* 2010, **2**, 1346–1371.

11 a) Y. Shvo, D. Czarkie, Y. Rahamim and D. F. Chodosh, *J. Am. Chem. Soc.* 1986, **108**, 7400–7402; b) J. S. M. Samec, and J.-E. Bäckvall, *Chem. Eur. J.* 2002, **8**, 2955–2961; c) D. Gnanamgari, A. Moores, E. Rajaseelan and R. H. Crabtree, *Organometallics* 2007, **26**, 1226–1230.

12 a) N. García, E. A. Jaseer, J. Munarriz, P. J. Sanz Miguel, V. Polo, M. Iglesias and L. A. Oro, *Eur. J. Inorg. Chem*. 2015, 4388–4395; b) A. Comas-Vives, G. Ujaque, A. Lledós, *THEOCHEM* 2009, **903**, 123–132. a) O. Pàmies, J.-E. Bäckvall, *Chem. Eur. J.* 2001, **7**, 5052–5058; b) A. Aranyos, G. Csjernyik, K. J. Szabó, J.-E. Bäckvall, *Chem. Commun.* 1999, 351–352; c) A. Comas-Vives, G. Ujaque, A. Lledós, *Organometallics* 2007, **26**, 4135–4144.

13 G. Giordano, R. H. Crabtree, R. M. Heintz, D. Forster and D. E. Morris, *Inorganic Synthesis Reagents for Transition Metal Complexes and Organometallic Synthesis,* 1990, **28**, 88–90.

14 M. J. Frisch, G. W. Trucks, H. B. Schlegel, G. E. Scuseria, M. A. Robb, J. R. Cheeseman, G. Scalmani, V. Barone, B. Mennucci, G. A. Petersson, H. Nakatsuji, M. Caricato, X. Li, H. P. Hratchian, A. F. Izmaylov, J. Bloino, G. Zheng, J. L. Sonnenberg, M. Hada, M. Ehara, K. Toyota, R. Fukuda, J. Hasegawa, M. Ishida, T. Nakajima, Y. Honda, O. Kitao, H. Nakai, T. Vreven, J. A. Montgomery Jr, J. E. Peralta, F. Ogliaro, M. Bearpark, J. J. Heyd, E. Brothers, K. N. Kudin, V. N. Staroverov, R. Kobayashi, J. Normand, K. Raghavachari, A. Rendell, J. C. Burant, S. S. Iyengar, J. Tomasi, M. Cossi, N. Rega, J. M. Millam, M. Klene, J. E. Knox, J. B. Cross, V. Bakken, C. Adamo, J. Jaramillo, R. Gomperts, R. E. Stratmann, O. Yazyev, A. J. Austin, R. Cammi, C. Pomelli, J. W. Ochterski, R. L. Martin, K. Morokuma, V. G. Zakrzewski, G. A. Voth, P. Salvador, J. J. Dannenberg, S. Dapprich, A. D. Daniels, ¨O. Farkas, J. B. Foresman, J. V. Ortiz, J. Cioslowski and D. J. Fox, Gaussian, Inc., Wallingford CT, 2013.

15 a) C. Lee, W. Yang and R. G. Parr, Phys. Rev. B., 1998, **37**, 785–789; b) A. D. Becke, J. Chem. Phys., 1993, **98**, 1372–1377; c) A. D. Becke, J. Chem. Phys., 1993, **98**, 5648–5652.

16 S. Grimme, J. Antony, S. Ehrlich and H. Krieg, J. Chem. Phys., 2010, **132**, 154104.

17 F. Weigend and R. Ahlrichs, Phys. Chem. Chem. Phys., 2005, **7**, 3297–3305.

18 J. Tomasi, B. Mennucci, R. Cammi, Chem. Rev., 2005, **105**, 2999–3094.